

Supporting Information

Enhanced capacitance of nitrogen-doped hierarchical porous carbide-derived carbon in matched ionic liquids

J.-K. Ewert,^a D. Weingarh,^b C. Denner,^a M. Friedrich,^a M. Zeiger,^c A. Schreiber,^b N. Jäckel,^c V. Presser,^{c*} and R. Kempe^{a*}

a) Inorganic Chemistry II, Universität Bayreuth, Universitätsstraße 30, NW I, 95440 Bayreuth, Germany

b) INM - Leibniz Institute for New Materials, Campus D2 2, 66123 Saarbrücken, Germany

c) Department of Materials Science and Engineering, Saarland University, Campus D2 2, 66123 Saarbrücken, Germany

* Corresponding authors. E-mail: kempe@uni-bayreuth.de (Rhett Kempe) and volker.presser@leibniz-inm.de (Volker Presser)

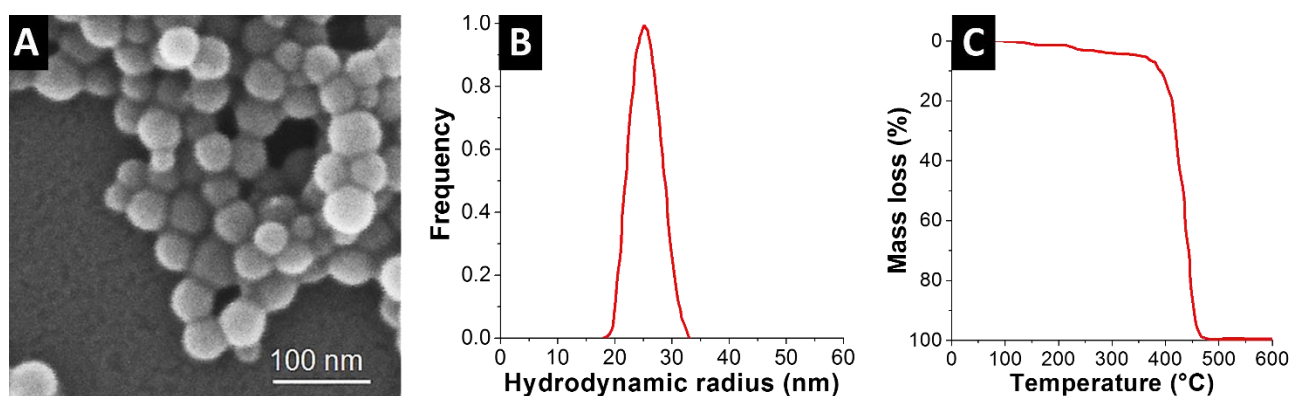


Figure S1. (A) Scanning electron micrograph of the polystyrene PS50. (B) Photon correlation spectrum of PS50 shows a narrow particle size distribution in the range of 19.7 nm and 31.3 nm with a peak at 24.8 nm. (C) Thermogravimetric analysis of PS50 shows a mayor mass loss between 400 and 470 °C (using a heating rate of 0.5 °C/min, nitrogen atmosphere).

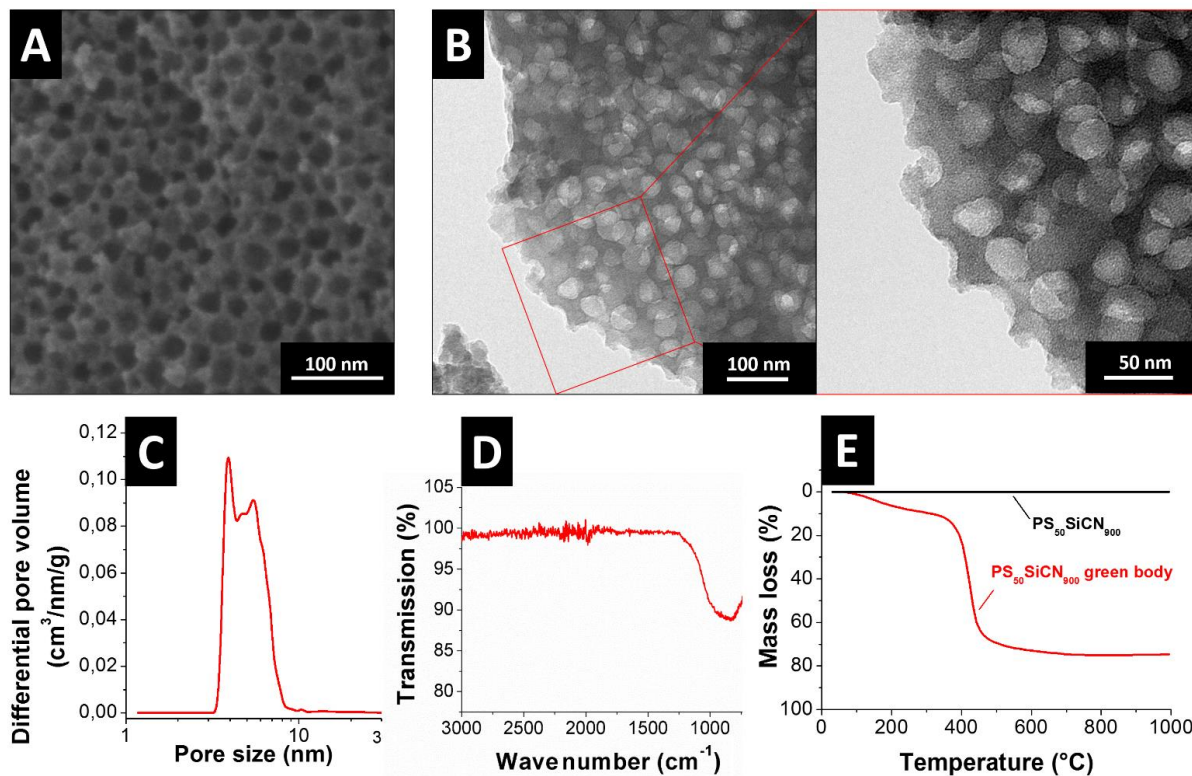


Figure S2. (A) SEM image and (B) TEM image of $\text{PS}_{50}\text{SiCN}_{900}$ verify the pore structure. (C) Pore size distribution of $\text{PS}_{50}\text{SiCN}_{900}$, measured by nitrogen gas sorption at -196°C , shows presence of mesopores and a BET surface area of $130\text{ m}^2/\text{g}$. (D) FT-IR measurement of $\text{PS}_{50}\text{SiCN}_{900}$ exhibits the characteristic broad SiCN peak between 1250 cm^{-1} and 750 cm^{-1} . (E) TGA measurements of the $\text{PS}_{50}\text{SiCN}_{900}$ green body and the $\text{PS}_{50}\text{SiCN}_{900}$ material.

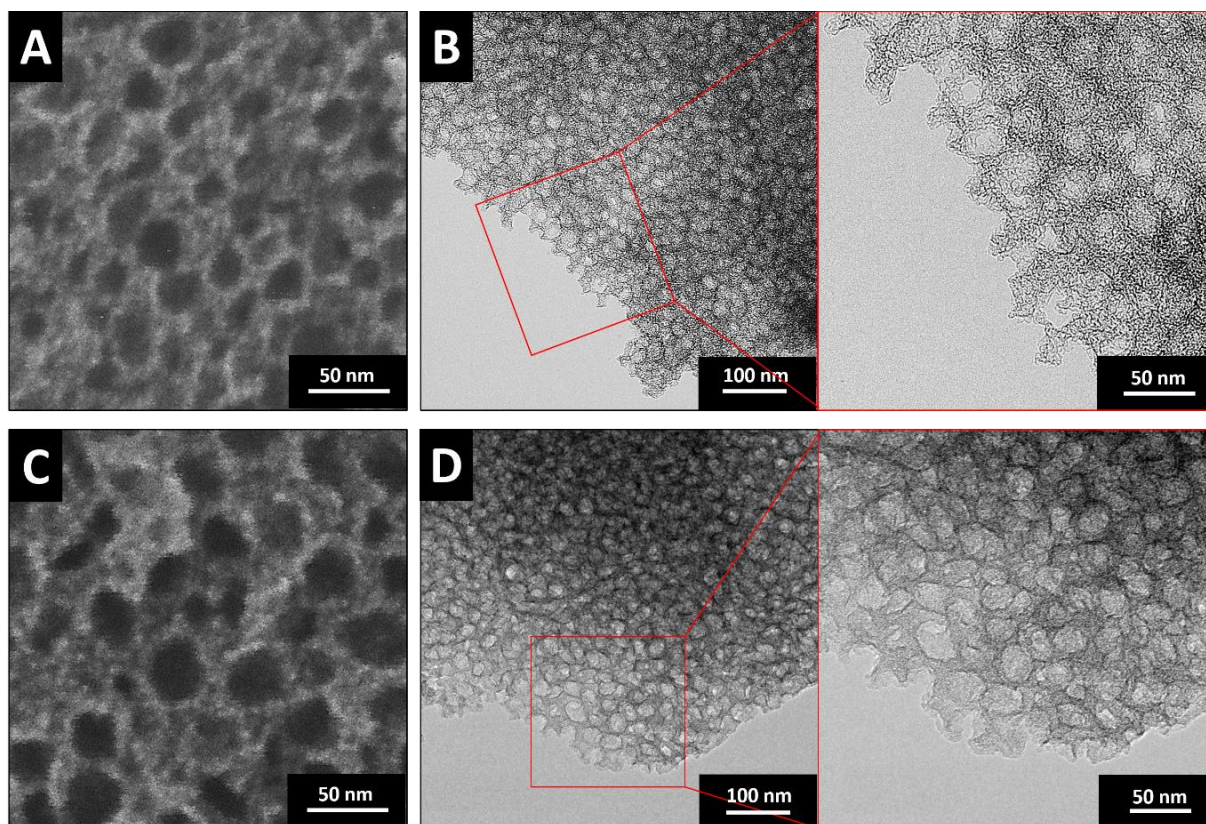


Figure S3. (A) SEM image and (B) TEM image of $\text{PS}_{50}\text{SiCN}_{900}\text{Cl}_2$ - 800°C . (C) SEM image and (D) TEM image of $\text{PS}_{50}\text{SiCN}_{900}\text{Cl}_2$ - 1000°C . Both materials show the honeycombed pore structure of the ceramic template.

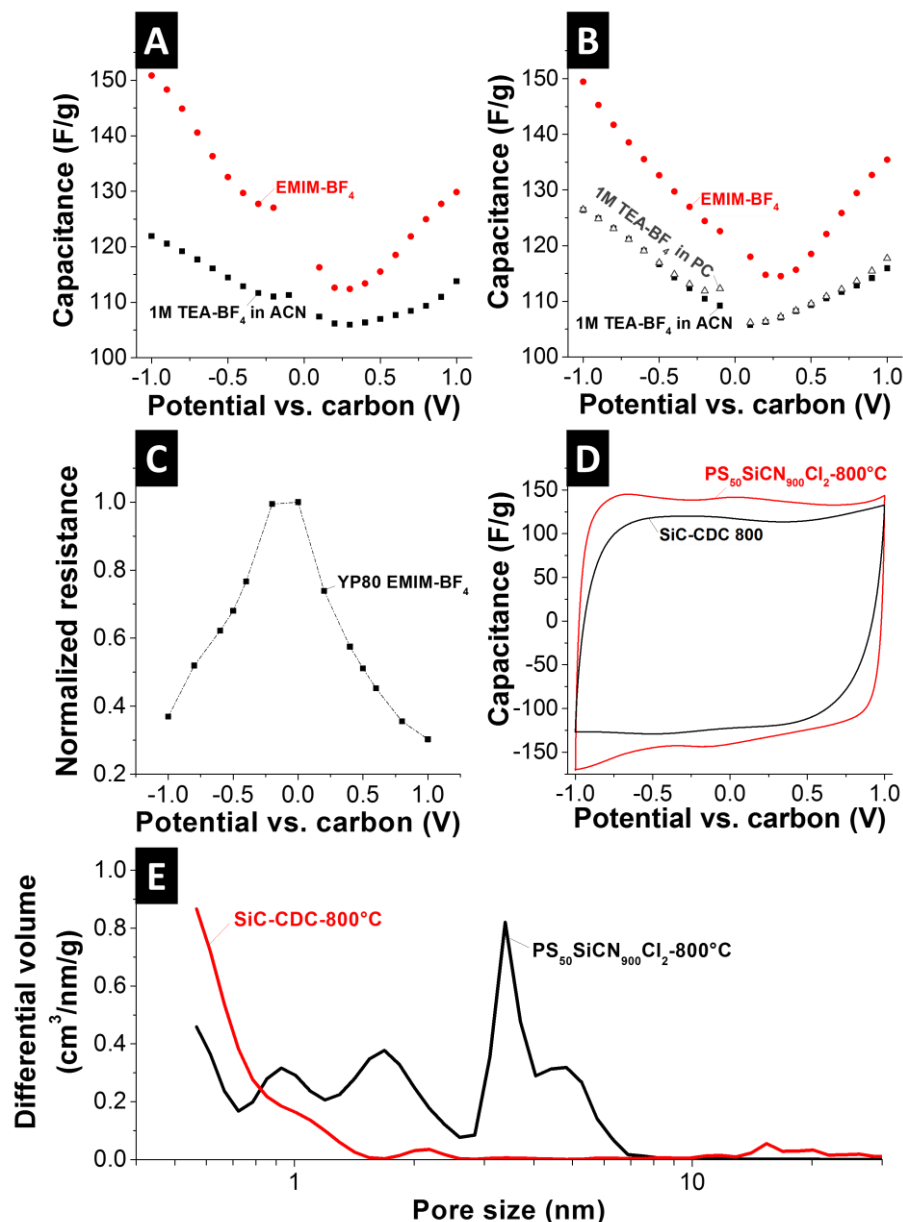


Figure S4. Comparison of the specific capacitance determined by GCPL for (A) $\text{PS}_{50}\text{SiCN}_{900}\text{Cl}_2-800^\circ\text{C}$ and (B) $\text{PS}_{50}\text{SiCN}_{900}\text{Cl}_2-1000^\circ\text{C}$. (C) In situ resistivity measurement of YP 80F with EMIM- BF_4 as electrolyte. (D) Cyclic voltammograms of SiC-CDC 800 and $\text{PS}_{50}\text{SiCN}_{900}\text{Cl}_2-800^\circ\text{C}$ in EMIM- BF_4 as electrolyte, scan rate: 10 mV/s. (E) Calculated pore size distribution of SiC-CDC 800°C and $\text{PS}_{50}\text{SiCN}_{900}\text{Cl}_2-800^\circ\text{C}$.

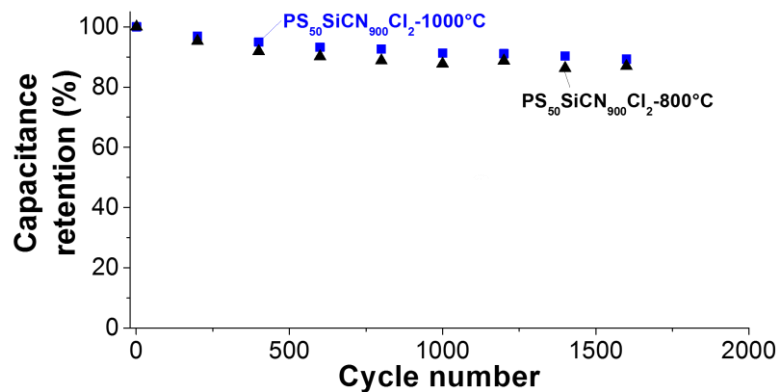


Figure S5. Cycling stability of $\text{PS}_{50}\text{SiCN}_{900}\text{Cl}_2-800^\circ\text{C}$ and $\text{PS}_{50}\text{SiCN}_{900}\text{Cl}_2-1000^\circ\text{C}$ in EMIM- BF_4 as electrolyte at 1 A/g.